

Orbital-Dependent Pseudogap Structure of an Al-Pd-Ru Quasicrystal Probed by X-ray Absorption and Core-Level Photoemission Spectroscopy

Nonoka U. Sakamoto^{1,2,*1,*2}, Hidenori Fujiwara^{1,2,3}, Takuya D. Nakamura^{1,2,*2}, Kenshin Okazaki^{1,2,*2}, Goro Nozue^{1,2,*3}, Takayuki Kiss¹, Yasumasa Takagi⁴, Souta Tanaka^{5,*4}, Yutaka Iwasaki⁶, Yasuhiro Niwa^{5,*4}, Asuka Ishikawa^{5,*5}, Takafumi D. Yamamoto⁵, Ryuji Tamura⁵, Akira Yasui⁴, Kiyofumi Nitta⁴, Satoru Hamamoto², Masaki Oura² and Akira Sekiyama^{1,2,3}

¹Division of Materials Physics, Graduate School of Engineering Science, The University of Osaka, Toyonaka 560-8531, Japan

²RIKEN SPring-8 Center, Sayo 679-5148, Japan

³Spintronics Research Network Division, Institute for Open and Transdisciplinary Research Initiatives, The University of Osaka, Suita 565-0871, Japan

⁴Japan Synchrotron Radiation Research Institute, Sayo 679-5198, Japan

⁵Department of Materials Science and Technology, Tokyo University of Science, Tokyo 125-8585, Japan

⁶National Institute for Materials Science, Tsukuba 305-0047, Japan

The unoccupied electronic states of Al-Pd-Ru quasicrystal (QC) have been investigated by X-ray absorption spectroscopy (XAS). In addition, the core-level peak binding energies have been verified by hard X-ray photoemission spectroscopy. From the comparison of the XAS spectra of the Al-Pd-Ru QC with those of single-element metals, the shift of the Al *K* edge can be explained by a shift in the Al 1s core level. In contrast, the shifts of the Pd and Ru *L*₃ edges cannot be explained solely by the shifts of the core levels. These differences are due to differences in the orbital-dependent partial density of states near the Fermi level. [doi:10.2320/matertrans.MT-MD2025012]

(Received November 4, 2025; Accepted February 21, 2026; Published April 25, 2026)

Keywords: quasicrystal, pseudogap, X-ray absorption spectroscopy, hard X-ray photoemission spectroscopy

1. Introduction

Al-based icosahedral quasicrystals (QCs) and their approximants have attracted attention for their thermoelectric properties due to suppression of the density of states (DOS) around the Fermi level (E_F), which is so called pseudogap structure [1, 2]. Therefore, many efforts have been made to enhance their thermoelectric properties [3–5]. Since semiconducting QCs with energy gaps are expected to show high thermoelectric performance, various systems have been surveyed for the discovery of them [6, 7]. Improving thermoelectric performance of the Al-based QCs requires enhancing Seebeck coefficient and electrical conductivity, both of which depend on the electronic structure in the vicinity of E_F . Therefore, direct observation of the electronic structure of the Al-based QCs is important for further investigations.

Understanding the electronic structure on the unoccupied side is just as important as that on the occupied side in Al-based quasicrystals. This insight is crucial for predicting changes in physical properties with increasing e/a (electrons per atom) ratio, for example. X-ray absorption spectroscopy (XAS) is powerful to investigate the orbital-selective unoccupied electronic states. However, examples of XAS studies on Al-based quasicrystals remain limited at present. In addition, discussions of the absorption-edge shifts must

account for shifts in the core level, yet such discussions have been largely absent to date. While Al-Pd-Re QCs, Al-Pd-Mn QCs and Al-Cu-Fe QCs have been the main targets for XAS study [8–10], observing the $2p$ levels of $5d$ TMs (Transition Metals) or the $1s$ levels of $3d$ TMs using photoemission spectroscopy is not easy due to their high binding energies. Study on Al-Pd- $4d$ TM QC has been suitable systems for this discussion since the binding energy of the $2p_{3/2}$ orbital in $4d$ TM is approximately 2–3.3 keV.

Recently Al-Pd-Ru QCs with the largest thermoelectric power factor $S^2\sigma$ of $780 \mu\text{W}/(\text{m}\cdot\text{K}^2)$ among QCs has been discovered [11]. The Al-Pd-Ru QC exhibits nonmetallic behavior in the temperature dependence of electrical conductivity [12], where the $\text{Al}_{71.5}\text{Pd}_{19}\text{Ru}_{9.5}$ QC is $\sim 360/(\Omega\cdot\text{cm})$ at ~ 300 K and $\sim 910/(\Omega\cdot\text{cm})$ at ~ 870 K. This is due to the deep pseudogap structure, which is directly observed by hard x-ray photoemission spectroscopy (HAXPES) in our previous study [13]. On the other hand, the unoccupied states above E_F remain still unclear, which is also important for improving the thermoelectric properties in future. Al *K*-edge XAS (Pd and Ru *L*₃-edge XAS) provides the information about unoccupied Al $3p$ (Pd and Ru $4d$) states owing to the dipole selection rule in the X-ray absorption process with the $1s \rightarrow 3p$ ($2p \rightarrow 4d$) transition.

In this paper, we report on the unoccupied Al $3p$, Pd and Ru $4d$ states of the Al-Pd-Ru QC investigated by the Al *K*-edge, Pd and Ru *L*₃-edge XAS. For Pd and Ru *L*₃-edge XAS, the spectra have been obtained in the total-electron-yield (TEY), partial-fluorescence-yield (PFY) and Transmission mode simultaneously on powder samples to evaluate the dependence on yield mode and the influence of the self-absorption effect. We have also performed the core-level HAXPES. The combination of the XAS and core-level

*1Corresponding author, E-mail: nsakamoto@decima.mp.es.osaka-u.ac.jp

*2Graduate Student, The University of Osaka

*3Present address: Physikalisches Institut und Würzburg-Dresden Cluster of Excellence ct.qmat, Julius-Maximilians-Universität, Würzburg, Germany

*4Graduate Student, Tokyo University of Science

*5Present address: Institute of Engineering Innovation, School of Engineering, The University of Tokyo

HAXPES allow us to reveal the orbital-dependent pseudogap structure, for which the gap would be opened for the Pd and Ru *d*-orbital partial density of states (PDOS) whereas the pseudogap is narrower for the Al sites.

2. Experimental Procedures

Polycrystalline sample of Al_{71.5}Pd₁₉Ru_{9.5} QC was prepared by the arc-melting method. The process of the synthesis has been described elsewhere [13]. As reference materials, the spectra of polycrystalline Al, Pd and Ru metals were also measured under the same conditions as those for the Al-Pd-Ru QC. All X-ray spectroscopic experiments described below were conducted at room temperature.

The Al *K*-edge XAS and photoemission spectroscopy (PES) for the Al-Pd-Ru QC and Al metal were performed at BL17SU in SPring-8 [14–16]. The XAS spectra were obtained in the TEY mode. The clean surface of the Al-Pd-Ru QC was obtained by fracturing *in situ*. The surface of the Al plate was scraped *in situ* with a diamond file. Surface cleanliness was checked with the weakness of the shoulder structure caused by the oxidation in PES spectra.

The Pd and Ru *L*₃-edge XAS measurements for the Al-Pd-Ru QC, Pd and Ru metals were performed at BL27SU in SPring-8 [17]. The experimental geometry is shown in Fig. 1. For the Al-Pd-Ru QC, bulk and powder samples were used. The bulk sample of the Al-Pd-Ru QC and the plate of Pd metal were polished in air. The Pd foil, the Ru plate and the powder sample of the Al-Pd-Ru QC were measured without surface treatment. The XAS spectra of the samples except for the powder sample were measured in PFY mode. The powder sample of the Al-Pd-Ru QC was uniformly covered onto the carbon tape and measured in PFY, TEY and transmission modes simultaneously. These three methods complement each other in probing depth, ensuring a reliable discussion [18]. The advantage of TEY and PFY mode is that the measurement can be performed on thick samples. The disadvantage of TEY is that it is relatively sensitive to surface conditions. PFY is relatively bulk-sensitive but can be affected by self-absorption effect or diffraction. In the Pd and Ru *L*₃-edge PFY-XAS, luminescence including Pd *L* α ₁ line and Ru *L* α ₁ line, respectively, were detected as signals using a silicon drift detector (SDD) with four channels.

The HAXPES measurements for the Al-Pd-Ru QC, Al, Pd and Ru metals were performed at BL09XU [19] in SPring-8 with SCIENTA OMICRON R4000 photoelectron spectrometer. The photon energy was set to 7.2 keV, and the overall energy resolution was set to 180 meV. The Fermi energy was determined by the Fermi edge of Au. The clean surface of the Al-Pd-Ru QC was obtained by fracturing *in situ* at the measuring temperature. The surface of the Al and Pd plates were scraped *in situ* with a diamond file. The Ru metal was evaporated onto Si(100) and then transferred to the measurement chamber after exposure to air. The thickness of the evaporated Ru layer is estimated to be about 65 nm by XRR (X-Ray Reflectivity) measurements. Sample cleanliness was checked with the weakness of the shoulder structure caused by the oxidation.

3. Results and Discussions

Figure 2 shows the Pd and Ru *L*₃-edge XAS spectra for the powder sample of the Al-Pd-Ru QC. The PFY- and TEY-XAS spectra were normalized by the intensity of the incident X-rays (*I*₀). The background signals have been subtracted from the TEY-XAS spectra. The spectra in the transmission mode are defined as $-\ln(I_1/I_0)$, where *I*₁ is the intensity of the transmitted X-rays. We have determined the absorption edge of each spectrum by the first inflection point (FIP). The FIP has been defined as the point where the second derivative of the spectrum becomes zero for the first time. The FIP of each spectrum is shown in Table 1. The difference of FIP is at most about ± 0.1 eV, indicating that differences in surface state or measurement mode have little influence for determining the absorption edges. Also note that the possible effect of the self absorption in the PFY mode can be included in the above difference of FIP as $< \pm 0.1$ eV. Furthermore, these differences are much smaller compared to the differences between the absorption edges of the Al-Pd-Ru QC and the reference single-element metals as discussed below.

Figure 3 shows the Al *K*-edge and Pd and Ru *L*₃-edge XAS spectra of the Al-Pd-Ru QC and reference single-element metals. The spectra were normalized by *I*₀ and then aligned by intensity in the EXAFS (Extended X-ray Absorption Fine Structure) region well above the absorption

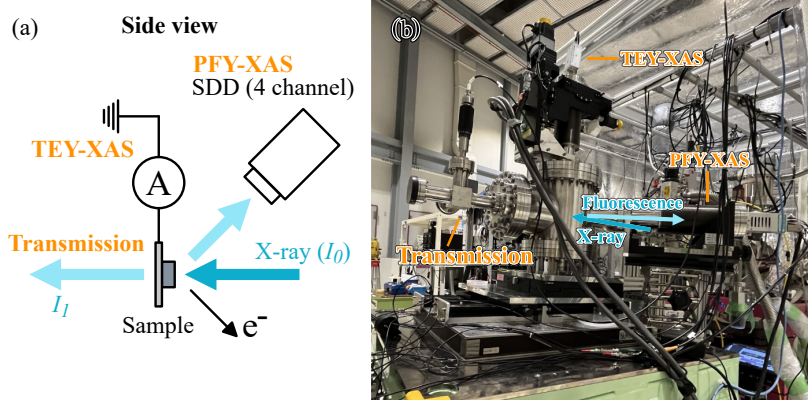


Fig. 1 (a) Experimental geometry for the XAS measurements in SPring-8 BL27SU. (b) Picture of the XAS instruments. (online color)

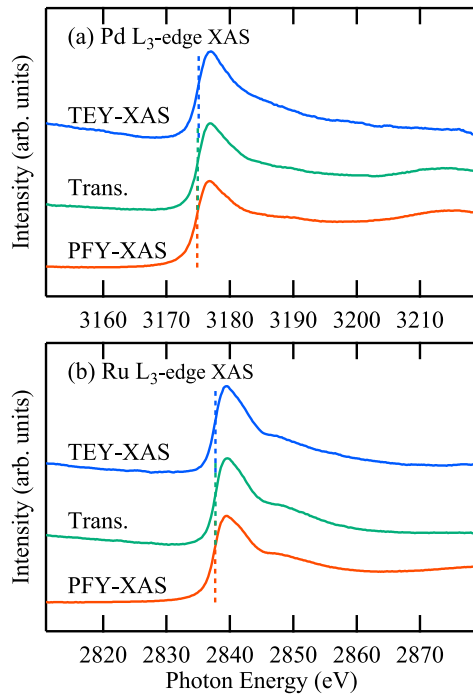


Fig. 2 (a) Pd and (b) Ru L_3 -edge XAS spectra of the powder Al-Pd-Ru QC in the TEY, Transmission (Trans.) and PFY modes. Each spectrum has been normalized by the intensity of the incident X-ray. The background signal has been subtracted from the TEY-XAS spectra. The dashed lines indicate the absorption edge determined by the first inflection point (FIP) for each spectrum. (online color)

Table 1 Values of the first inflection point (FIP) determined as the absorption edge for each XAS spectrum of the powder Al-Pd-Ru QC in Fig. 2.

	FIP (eV)	
	Pd L_3 -edge	Ru L_3 -edge
TEY-XAS	3175.09	2837.72
Transmission	3174.96	2837.71
PFY-XAS	3174.83	2837.67

edge. When we compare the spectra of the bulk Al-Pd-Ru QC with those of the powder QC, it is found that the difference of the spectra is negligible between the bulk and powder. The absorption edges of the Al-Pd-Ru QC shifts to higher energy than those of single-element metals. This tendency, where the absorption edges of a QC are observed at higher energy sides than those of simple metals in all XAS spectra, has also been reported for the Al-Pd-Re QCs [10] with deep pseudogap structures [20]. The relative absorption-edge shifts are estimated as 0.5 eV and 0.6 eV for the Al K and Ru L_3 edges, respectively. In contrast, the shift is relatively large as 3.1 eV at the Pd L_3 edge. This difference is larger than the difference between Pd metal and Pd(II) oxide [21]. On the other hand, the absorption-edge shift originates from both unoccupied partial density of states and core levels to be excited. For discussion of the difference in the absorption-edge shifts, it is necessary to investigate the core levels of the Al-Pd-Ru QC and single-element metals.

Figure 4 shows the Al $1s$, Pd and Ru $2p_{3/2}$ core-level HAXPES spectra of the Al-Pd-Ru QC and reference single-

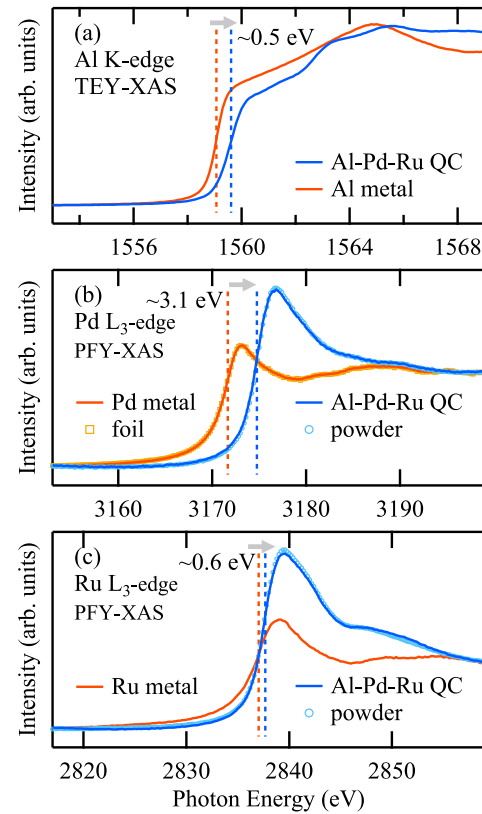


Fig. 3 (a) Al K -edge TEY-XAS, (b) Pd and (c) Ru L_3 -edge PFY-XAS spectra of the Al-Pd-Ru QC and reference single-element metals. The dashed lines indicate the absorption edge determined by FIP of each spectrum. The gray arrows indicate the direction of the absorption-edge shift in the XAS spectra of the Al-Pd-Ru QC compared with those of the single-element metals. (online color)

element metals. The shoulder structure observed around ~ 2 eV higher binding energy side from the main peak in Fig. 4(a) was caused by the oxidation. Even as surface oxidation progresses, the main peak binding energy has been hardly shifted. The Al $1s$ and Pd $2p_{3/2}$ core-level peaks of the Al-Pd-Ru QC are shifted toward the higher binding energy side by about 0.2 eV and 2.0 eV, respectively, compared to those of the simple metals. On the other hand, the Ru $2p_{3/2}$ core-level peak of the Al-Pd-Ru QC is located on the lower binding energy side by about 0.4 eV compared to that of the Ru metal. The different tendency of the peak shifts would reflect the degree of the charge transfer among the sites as pointed out elsewhere [13]. Possible intrinsic charge-transfer satellite structure due to electron correlations is not seen in all core-level HAXPES spectra, which indicates that the core-level peak binding energy directly reflects the core level energy.

In order to discuss the unoccupied electronic states near E_F based on the XAS spectra, we need to take both shifts of the absorption edge in the XAS spectra and the core-level peak in the HAXPES spectra, which has been lacking in previous studies, into account. When Δ is defined as the difference between the absorption edge and the peak binding energy E_B to be excited, it is evaluated as about -0.5 , -2.3 and -1.7 eV for the Al, Pd and Ru sites of the single-element metals from Table 2. These negative values are due to the attractive Coulomb interactions between the outer valence electrons

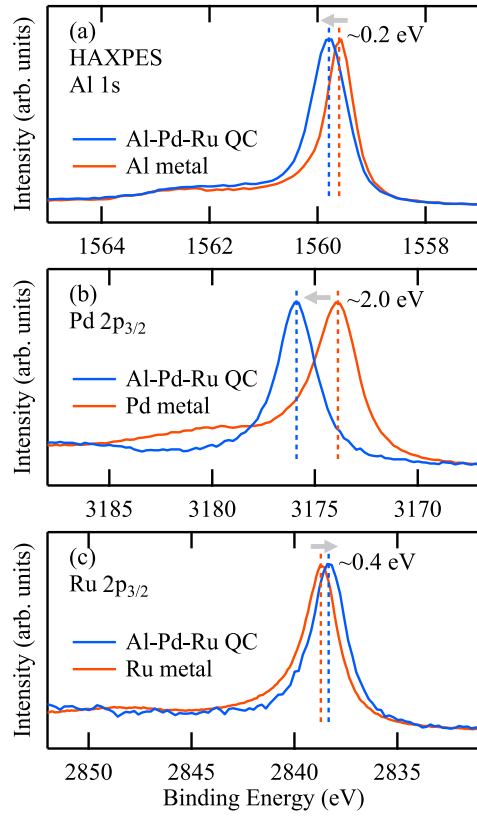


Fig. 4 (a) Al $1s$, (b) Pd $2p_{3/2}$ and (c) Ru $2p_{3/2}$ core-level HAXPES spectra of the Al-Pd-Ru QC and reference single-element metals. The dashed lines indicate main peak binding energies (E_B). The gray arrows indicate the directions of shift for the main peaks in the HAXPES spectra of the Al-Pd-Ru QC relative to that of the single-element metals. (online color)

(including excited electrons) and the core hole created in the X-ray absorption process. If these attractive Coulomb interactions were negligible, $\Delta = 0$ eV would be expected for conventional metals. Note that the attractive Coulomb interactions depend on element and orbital but are essentially independent on material since these are intraatomic quantities. On the other hand, Δ is estimated from Table 2 as about -0.2 , -1.2 and -0.7 eV for the Al, Pd and Ru sites of the Al-Pd-Ru QC. Thus, the differences in Δ between the Al-Pd-Ru QC and single-element metals are evaluated as ~ 0.3 eV for the Al sites and ~ 1 eV for the Pd and Ru sites.

Table 2 Values of the absorption edge of the XAS spectra in Fig. 3 and main peak binding energies (E_B) in the HAXPES spectra in Fig. 4. These values have been obtained from the spectra for the bulk samples. The error of the core-level peak fitting is ~ 0.03 eV.

	Absorption edge (eV)	Peak E_B (eV)
	Al K -edge	Al $1s$
Al-Pd-Ru QC	1559.61	1559.79
Al metal	1559.07	1559.60
	Pd L_3 -edge	Pd $2p_{3/2}$
Al-Pd-Ru QC	3174.74	3175.90
Pd metal	3171.64	3173.89
	Ru L_3 -edge	Ru $2p_{3/2}$
Al-Pd-Ru QC	2837.67	2838.34
Ru metal	2837.03	2838.72

When we assume that the element-dependent attractive Coulomb interactions are essentially equivalent between the QC and single-element metals, the differences in Δ reflect the pseudogap electronic structure in the unoccupied side for the Al-Pd-Ru QC.

Figure 5 summarizes the element-dependent energy-level diagrams of the Al-Pd-Ru QC compared to those of the single-element metals based on our XAS and core-level HAXPES results. In the Pd and Ru sites, the $2p \rightarrow 4d$ transitions to the absorption edges correspond to the transitions to the $4d$ unoccupied states at ~ 1 eV above E_F for the Al-Pd-Ru QC while those are due to the transitions to the unoccupied states at E_F for the single-element metals. This indicates the opening of the pseudogap in the $4d$ PDOS

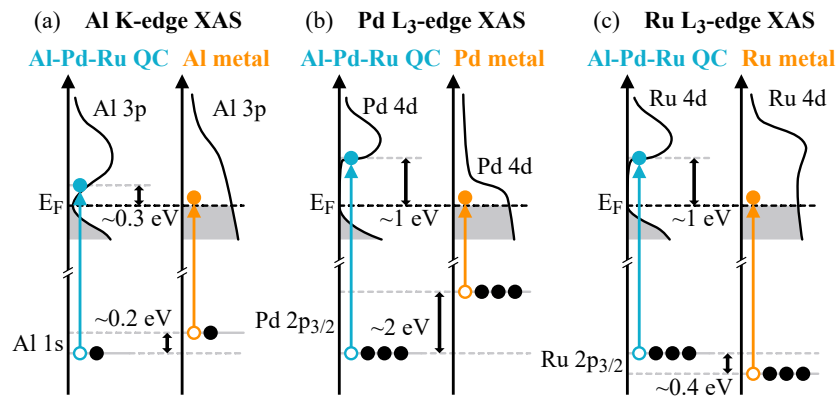


Fig. 5 Schematic energy-level diagrams of (a) Al $1s \rightarrow 3p$, (b) Pd $2p_{3/2} \rightarrow 4d$ and (c) Ru $2p_{3/2} \rightarrow 4d$ transitions in the Al-Pd-Ru QC and reference single-element metals. (online color)

near E_F for the Al-Pd-Ru QC. In the Al sites, the $1s \rightarrow 3p$ transitions to the absorption edge are due to the $3p$ unoccupied state at ~ 0.3 eV above E_F for the Al-Pd-Ru QC, which suggests the narrower pseudogap states. These mean that the Al $3p$ states contribute predominantly to the DOS near E_F while the Pd and Ru $4d$ contributions are much less near E_F , which is consistent with the finding obtained from our previous study for the occupied electronic states of the Al-Pd-Ru QC [13]. Although the precise discussion on the pseudogap electronic structure in a meV scale is difficult from the XAS spectra of which the lifetime broadening is of the order of 1 eV, we can clarify the orbital-dependent pseudogap electronic structure of the Al-Pd-Ru QC from the XAS and core-level HAXPES spectra compared to those of the single-element metals as discussed here.

Our results show that analysis of the XAS spectrum of Al-based QCs requires consideration of both core-level shifts and unoccupied states since the suppression of the PDOS near E_F affects the absorption-edge shift in the XAS spectra as we have discussed here. In addition, the bottom of the pseudogap structure of the Al-Pd-Ru QC is largely ascribed by the Al sites. Identifying the origin of this residual Al state and controlling it would be important for improving thermoelectric performance of the Al-Pd-Ru QCs.

4. Conclusion

We have performed the XAS and HAXPES of the Al-Pd-Ru QC and the Al, Pd and Ru metals. In the XAS, the absorption edges in the spectra of the Al-Pd-Ru QC have been all observed at the higher energy side compared to those of the simple metals. The shift in the core-level peaks in the HAXPES have shown the different tendency depending on element. We have concluded that this difference is due to the difference in the contribution from each site to DOS near the E_F in the Al-Pd-Ru QC.

Acknowledgements

We acknowledge Y. Torii, M. Sakaguchi, S. Kaneko and M. Togawa for supporting the experiments. The XAS experiments at BL27SU and BL17SU in SPring-8 were performed under the approvals of JASRI (Proposal No. 2024B1957) and RIKEN (Proposal No. 20250096), respectively. The HAXPES experiment at BL09XU in SPring-8 was performed under the approvals of JASRI (Proposal. Nos. 2024B1899 and 2025A1986). This work was financially supported by a Grant-in-Aid for Innovative Areas (JP22H04594), a Grant-in-Aid for Transformative Research (JP23H04867), a Grant-in-Aid for Scientific Research (JP22K03527 and JP24K03202), from JSPS and MEXT, Japan, and CREST (JPMJCR22O3) from JST, Japan. This work was also supported by the Thermal & Electric Energy Technology Foundation, Japan. G. Nozue was supported by the Osaka University fellowship program of Super Hierarchical Materials Science Program and by the JSPS Research Fellowship for Young Scientists.

REFERENCES

- [1] K. Kirihaara and K. Kimura: Covalency, semiconductor-like and thermoelectric properties of Al-based quasicrystals: icosahedral cluster solids, *Sci. Technol. Adv. Mater.* **1** (2000) 227–236.
- [2] K. Kirihaara, T. Nagata, K. Kimura, K. Kato, M. Takata, E. Nishibori and M. Sakata: Covalent bonds and their crucial effects on pseudogap formation in α -Al(Mn,Re)Si icosahedral quasicrystalline approximant, *Phys. Rev. B* **68** (2003) 014205.
- [3] K. Kirihaara and K. Kimura: Composition dependence of thermoelectric properties of AlPdRe icosahedral quasicrystals, *J. Appl. Phys.* **92** (2002) 979–986.
- [4] T. Nagata, K. Kirihaara and K. Kimura: Effect of Ru substitution for Re on the thermoelectric properties of AlPdRe icosahedral quasicrystals, *J. Appl. Phys.* **94** (2003) 6560–6565.
- [5] Y. Takagiwa, T. Kamimura, S. Hosoi, J.T. Okada and K. Kimura: Thermoelectric properties of polygrained icosahedral $\text{Al}_{71-x}\text{Ga}_x\text{Pd}_{20}\text{Mn}_9$ ($x = 0, 2, 3, 4$) quasicrystals, *J. Appl. Phys.* **104** (2008) 073721.
- [6] Y. Iwasaki, K. Kitahara and K. Kimura: Experimental realization of a semiconducting quasicrystalline approximant in Al-Si-Ru system by band engineering, *Phys. Rev. Mater.* **3** (2019) 061601(R).
- [7] Y. Iwasaki, K. Kitahara and K. Kimura: Effects of Cu doping on thermoelectric properties of Al-Si-Ru semiconducting quasicrystalline approximant, *Phys. Rev. Mater.* **5** (2021) 125401.
- [8] O. Polozhentsev, M. Bryleva, A. Kravtsova, V. Kochkina and A. Soldatov: Icosahedral phase formation in an Al-Cu-Fe quasicrystal, *Bull. Russ. Acad. Sci., Physics* **79** (2015) 1173–1179.
- [9] E. Belin, Z. Dankhazi, A. Sadoc and J.M. Dubois: Electronic distributions in quasicrystalline Al-Pd-Mn alloys, *J. Phys. Condens. Matter* **6** (1994) 8771–8780.
- [10] Y.Y. Lay, J.C. Jan, J.W. Chiou, H.M. Tsai, W.F. Pong, M.-H. Tsai, T.W. Pi, J.F. Lee, C.I. Ma, K.L. Tseng, C.R. Wang and S.T. Lin: Observation of metal-insulator transition in Al-Pd-Re quasicrystals by x-ray absorption and photoemission spectroscopy, *Appl. Phys. Lett.* **82** (2003) 2035–2037.
- [11] Y. Iwasaki: unpublished.
- [12] R. Tamura, T. Asao, M. Tamura and S. Takeuchi: Ordered Al-Pd-Ru icosahedral quasicrystal and its crystalline approximants and their electrical resistivities, *J. Phys. Condens. Matter* **11** (1999) 10343–10352.
- [13] N.U. Sakamoto *et al.*: submitted; arXiv:2505.11156.
- [14] H. Ohashi *et al.*: Performance of a Highly Stabilized and High-resolution Beamline BL17SU for Advanced Soft X-ray Spectroscopy at SPring-8, *AIP Conf. Proc.* **879** (2007) 523–526.
- [15] Y. Senba, H. Ohashi, H. Kishimoto, T. Miura, S. Goto, S. Shin, T. Shintake and T. Ishikawa: Fundamental Techniques for High Photon Energy Stability of a Modern Soft X-ray Beamline, *AIP Conf. Proc.* **879** (2007) 718–721.
- [16] T. Tanaka, T. Seike, A. Kagamiyama, H. Aoyagi, T. Kai, M. Sano, S. Takahashi and M. Oura: Development of an insertion device selectively operational as a helical/figure-8 undulator, *J. Synchrotron Radiat.* **30** (2023) 301–307.
- [17] T. Tanaka, T. Hara, M. Oura, H. Ohashi, H. Kimura, S. Goto, Y. Suzuki and H. Kitamura: Construction and performance of a figure-8 undulator, *Rev. Sci. Instrum.* **70** (1999) 4153–4160.
- [18] F. de Groot and A. Kotani: *Core Level Spectroscopy of Solids*, (CRC Press, Boca Raton, 2008).
- [19] A. Yasui, Y. Takagi, T. Osaka, Y. Senba, H. Yamazaki, T. Koyama, H. Yumoto, H. Ohashi, K. Motomura, K. Nakajima, M. Sugahara, N. Kawamura, K. Tamasaku, Y. Tamenori and M. Yabashi: BL09XU: an advanced hard X-ray photoelectron spectroscopy beamline of SPring-8, *J. Synchrotron Radiat.* **30** (2023) 1013–1022.
- [20] S. Sarkar, M. Krajčí, P. Sadhukhan, V.K. Singh, A. Gloskovskii, P. Mandal, V. Fournée, M.-C. de Weerd, J. Ledieu, I.R. Fisher and S. Roy Barman: Anderson localization of electron states in a quasicrystal, *Phys. Rev. B* **103** (2021) L241106.
- [21] H.A. Suarez Orduz, L. Bugarin, S.-L. Heck, P. Dolcet, M. Casapu, J.-D. Grunwaldt and P. Glatzel: L_3 -edge X-ray spectroscopy of rhodium and palladium compounds, *J. Synchrotron Radiat.* **31** (2024) 733–740.